HHS Public Access

Author manuscript

Pathog Dis. Author manuscript; available in PMC 2015 January 11.

Published in final edited form as:

Pathog Dis. 2013 October ; 69(1): 36–48. doi:10.1111/2049-632X.12063.

Analysis of the *Staphylococcus aureus* abscess proteome identifies antimicrobial host proteins and bacterial stress responses at the host-pathogen interface

Ahmed S. Attia[1,5,#], **James E. Cassat**[4,#], **Sheg O. Aranmolate**[1], **Lisa J. Zimmerman**[3], **Kelli L. Boyd**[1,2], and **Eric P. Skaar**[1,*]

[1]Department of Pathology, Microbiology, and Immunology, Vanderbilt University Medical Center, Nashville, TN 37232

[2]Division of Animal Care, Vanderbilt University Medical Center, Nashville, TN 37232

[3]Department of Biochemistry and Jim Ayers Institute for Precancer Detection and Diagnosis, Vanderbilt University Medical Center, Nashville, TN 37232

[4]Division of Pediatric Infectious Diseases, Department of Pediatrics, Vanderbilt University Medical Center, Nashville, TN 37232

[5]Department of Microbiology and Immunology, Faculty of Pharmacy, Cairo University, Cairo, Egypt 11562

Abstract

Abscesses are a hallmark of invasive staphylococcal infections and the site of a dynamic struggle between pathogen and host. However, the precise host and bacterial factors that contribute to abscess formation and maintenance have not been completely described. In this work, we define the *Staphylococcus aureus* abscess proteome from both wildtype and neutropenic mice to elucidate the host response to staphylococcal infection and uncover novel *S. aureus* virulence factors. Among the proteins identified, the mouse protein histone H4 was enriched in the abscesses of wildtype compared to neutropenic animals. Histone H4 inhibits staphylococcal growth *in vitro* demonstrating a role for this protein in the innate immune response to staphylococcal infection. These analyses also identified staphylococcal proteins within the abscess, including known virulence factors and proteins with previously unrecognized roles in pathogenesis. Within the latter group was the universal stress protein Usp2, which was enriched in kidney lesions from neutropenic mice and required for the *S. aureus* response to stringent stress. Taken together, these

*Corresponding Author: Mailing address: Eric P. Skaar, Department of Pathology, Microbiology, and Immunology, Vanderbilt University School of Medicine, 1161 21st Avenue South, MCN A-5102, Nashville, TN 37027., Phone: (615)-343-0002., Fax: (615)-343-7392., eric.skaar@vanderbilt.edu.

#A.S.A and J.E.C. contributed equally to this work.

Author Contributions

Conceived and designed the experiments: ASA, JEC, EPS.
Performed the experiments: ASA, JEC, SOA, LJZ.
Analyzed the data: ASA, JEC, LJZ, KLB, EPS.
Contributed reagents/materials/analysis tools: ASA, JEC LJZ, KLB, EPS.
Wrote the paper: ASA, JEC, EPS.

data describe the *S. aureus* abscess proteome and lay the foundation for the identification of contributors to innate immunity and bacterial pathogenesis.

Keywords

Proteomics; *S. aureus*; pathogenesis; innate immunity

Introduction

Staphylococcus aureus is a Gram-positive bacterium and a member of the vertebrate microbiome, colonizing approximately 30% of the human population. Paradoxically, this organism is highly virulent, capable of causing a diverse array of infections [1]. These range from minor skin infections to more serious invasive diseases that are responsible for considerable morbidity and mortality [1,2]. The significant public health burden of staphylococcal infections is underscored by the fact that *S. aureus* is responsible for approximately 40,000 deaths in the United States per year [2]. Methicillin resistant *S. aureus* (MRSA) infections are prevalent within both the health care setting and the community (CA-MRSA), highlighting the necessity to identify molecular targets for the development of new therapeutics.

Upon breaching the initial sites of colonization, *S. aureus* can infect virtually any organ leading to the rapid recruitment of host neutrophils and macrophages. This inflammatory response promotes cell death and tissue destruction. In response to the offending microbe, the host produces fibrin deposits which confine *S. aureus* and necrotic tissue into what is known as an abscess [3]. Abscess formation is a hallmark of staphylococcal infection that protects the host from bacterial metastasis and the spread of infection to neighboring tissue sites.

As a focal point in the host-pathogen interface, the abscess contains host defense molecules that are essential to confine bacterial infection and prevent spread. Concurrently, bacteria within the abscess express proteins that are critical to their survival within this hostile host environment. To identify host and bacterial proteins that are abundant at this infectious interface, we performed a proteomic analysis of murine kidney abscesses from *S. aureus* infected animals. Proteomic analyses were performed on both wildtype and neutropenic animals in an effort to determine the contribution of neutrophils to the abscess proteome. Collectively, these experiments define the *S. aureus* abscess proteome and identify host and bacterial contributors to the host-pathogen interface.

Results

Neutrophil depletion results in large disorganized renal lesions

To determine the contribution of neutrophils to the proteome of *S. aureus* kidney abscesses, it was first necessary to establish an infection model of neutropenic mice. C57BL/6J mice were treated with either the neutrophil depleting anti-Gr1 antibody RB6 [4,5], or the isotype control antibody SRF3 [6], followed by intravenous injection with wildtype *S. aureus* strain Newman (NW). Ninety-six hours following infection, mice were euthanized and the kidneys

were removed for analysis. Decreased myeloperoxidase immunoreactivity in the kidneys indicated that the RB6 treatment was successful in diminishing the neutrophilic response (Fig. 1), consistent with previous flow cytometry analyses of infected kidneys from RB6-treated mice [6]. In the SRF3-treated mouse, the inflammation expanded beyond the renal parenchyma and filled the renal capsule (Fig. 1A) while in the RB6-treated mouse, the response was dramatically diminished (Fig. 1B). H & E staining of the respective sections revealed that in the SRF3-treated mouse, the inflammatory infiltrate consisted of neutrophils and macrophages forming densely packed sheets encircling the bacterial aggregations (Fig. 1C and E). Within these inflammatory foci, bacterial aggregates were small and their spread was limited. In contrast, in an RB6-treated mouse, bacterial growth was florid and leukocyte numbers were markedly decreased. Therefore, in the absence of neutrophils, the host response is ineffective at forming organized structures that contain staphylococcal infection (Fig. 1D and F).

Proteomic analysis of the staphylococcal abscesses

We sought to define the abscess proteome and evaluate the contribution of neutrophils to the protein composition of the abscess. To this end, abscessed or lesioned tissues from representative SRF3-treated (wildtype) and RB6-treated (neutropenic) mice were subjected to proteomic analysis using shotgun techniques as described in Materials and Methods. We identified 235 mouse proteins and 14 *S. aureus* proteins within the abscesses from a wildtype animal and 266 mouse proteins and 22 *S. aureus* proteins within the abscesses from a neutropenic animal with a total of 315 mouse proteins and 22 staphylococcal proteins (Summarized in Table 1). Approximately 12% of the detected mouse proteins were more abundant in the neutropenic animal while another approximately 12% were more abundant in the mouse with an intact neutrophil population. The sample size of this analysis does not allow for rigorous statistical comparisons. Instead, the experiment was designed to provide a qualitative assessment of the protein composition of the abscess. This data set lays the foundation for the identification of host and bacterial factors that contribute to the outcome of systemic staphylococcal infection.

Mouse proteins within the abscess that change abundance upon neutrophil depletion

Forty mouse proteins were less abundant in neutropenic lesions as compared to neutrophil rich abscesses (Table 2). As expected, neutrophil associated proteins such as myeloid bactenecin (neutrophilic granule protein), lactotransferrin precursor, myeloperoxidase, and neutrophil gelatinase-associated lipocalin precursor (NGAL) were among the proteins exhibiting the most substantial decrease in abundance following neutrophil depletion. Other classes of proteins exhibiting decreased abundance upon neutrophil depletion include components of the cytoskeleton, extracellular matrix (ECM) proteins, antioxidants, and histones. This abundance pattern likely reflects the decreased tissue damage observed in infected mice that have been depleted of neutrophils. Thirty-eight proteins exhibited an increase in abundance upon neutrophil depletion (Table 3). These included a large number of proteins involved in the clotting cascade and coenzyme A (CoA) synthesis. Taken together, these results demonstrate the impact of neutrophils on the staphylococcal abscess proteome and identify candidate host proteins involved in protection against microbial infection.

The abundance of histone H4 is markedly decreased upon neutrophil depletion

Histones are eukaryotic proteins of the nucleus that contribute to chromatin formation and transcriptional regulation [7]. However, histones have also been implicated in innate immunity [8,9,10]. Histones are involved in the formation of neutrophil extracellular traps (NETs) that bind bacteria and ensure a high local concentration of antimicrobial agents to degrade bacterial virulence factors and kill invading pathogens [11,12]. The abscess proteome revealed that unique spectra corresponding to histone H4 were detected at approximately half the levels in a neutropenic mouse as compared to a mouse with a robust neutrophil response. To validate this observation, abscessed tissue sections from wildtype and neutropenic mice were immunohistochemically stained with antisera specific for histone H4. Examination of the immunolabeled sections revealed increased extracellular histone H4 in proximity to the staphylococcal bacterial aggregates in kidney abscesses of wildtype mice (Fig. 2A). In contrast, neutropenic lesions had fewer infiltrating cells, very little extracellular histone H4, and large bacterial aggregates (Fig. 2B). The abundance of histone H4 surrounding the bacteria indicates that this protein may contribute to defense against staphylococcal infection. To test this hypothesis, *S. aureus* were cultured in the presence of increasing concentrations of purified human histone H4. *S. aureus* growth was inhibited in a dose-dependent manner by purified histone H4, suggesting that extracellular histone H4 may be directly antimicrobial during infection (Fig. 3). Taken together, these data show that histone H4 is abundant in the staphylococcal abscess in a neutrophil-dependent manner, and exhibits antibacterial activity against *S. aureus*.

S. aureus proteins within the abscess that change abundance upon neutrophil depletion

There are numerous technical challenges associated with the detection of bacterial proteins within infected tissue, thus only 22 staphylococcal proteins were detected within abscesses of *S. aureus* infected mice. The detected bacterial proteins likely represent proteins that are highly abundant within staphylococcal lesions. Among these proteins, thirteen were more abundant in the neutropenic mice including secreted virulence factors (LukD, LukE, LukS, HlgB, HlgC, MapN/Eap, and Ssp/Emp), proteins involved in iron acquisition (IsdA), and proteins involved in glycolysis/gluconeogenesis (Adh1, Ldh, Eno, GapA) (Table 4). In addition, a protein belonging to the universal stress protein (Usp) superfamily was more abundant upon neutrophil depletion. Detection of this uncharacterized Usp protein, which is presumably produced in high abundance in kidney lesions, indicates that this protein might contribute to the interaction between *S. aureus* and the vertebrate host. It is important to note that the increased abundance of these proteins in the lesions of neutropenic mice might be due to either increased bacterial yield, or an increased abundance of these gene products in the absence of neutrophils. It is not possible to distinguish between these two possibilities using the proteomic analyses employed here.

Usp2 is growth phase regulated

The genome of *S. aureus* strain Newman contains two genes predicted to encode for proteins belonging to the universal stress protein superfamily (*NWMN_1600* and *NWMN_1604*). We designated the protein encoded by *NWMN_1600* as Usp1 and the protein encoded by *NWMN_1604* as Usp2 in keeping with their genomic localization. Using this nomenclature,

Usp2 was the protein detected within the staphylococcal lesions. Our ability to detect Usp2 within lesioned tissue from neutropenic mice implies that this protein is abundant at the infectious focus. To investigate the regulation of *usp2* expression, a *xylE* transcriptional reporter was constructed and cells carrying the reporter either with or without the *usp2* promoter were assayed at different growth phases. At mid-logarithmic phase the *usp2* promoter showed XylE activity approximately 100-fold higher than the control vector indicating that *usp2* is abundantly transcribed at this growth stage. Moreover, entrance into late-logarithmic/early stationary phase resulted in a further 100-fold increase in expression (Fig. 4). Collectively, these results suggest that *usp2* is regulated in a growth phase dependent manner, with the highest expression levels observed in late-logarithmic/early stationary phase.

Usp2 is involved in the stringent stress response

Protein sequence alignments indicated that *S. aureus* Usp2 contains a Usp-like conserved domain (cd00293) [13]. Proteins belonging to this super family are involved in responding to a variety of stressors [14,15]. The presence of a Usp-like domain and the sequence similarity between this protein and Usp proteins from other organisms suggests that *S. aureus* Usp2 may play a role in the staphylococcal stress response. To test this hypothesis, we evaluated the effect of the stringent stress inducer mupirocin on *usp2* expression and *S. aureus* growth. Mupirocin is an antimicrobial agent that induces the bacterial stringent response by inhibiting isoleucyl tRNA synthetase, thereby increasing the cellular concentration of uncharged $tRNA^{Ile}$ molecules [16]. Anderson *et al.* have shown that *usp2* is transcriptionally induced upon exposure to sub-inhibitory concentrations of mupirocin in the *S. aureus* strain UAMS-1 [17]. To validate these findings in the *S. aureus* Newman strain background, a *usp2-gfp* reporter was exposed to sub-inhibitory concentrations of mupirocin. Treatment with mupirocin induced the expression of *usp2,* as indicated by an increase in detectable fluorescence (Fig. 5A). To determine if Usp2 is required for overcoming the inhibitory effect of mupirocin, a deletion mutation of the *usp2* gene was constructed (Δ*usp2*) and tested for survival in the presence of inhibitory concentrations of mupirocin. These experiments revealed an approximately 50% decrease in the survival rate of Δ*usp2* as compared to wildtype *S. aureus* when treated with mupirocin (Fig. 5B). The observed decreased survival was despite the fact that Δ*usp2* grows similarly to wildtype *S. aureus* in rich medium (data not shown). This increase in susceptibility to mupirocin was reversed by providing a full length copy of *usp2 in trans,* confirming that the absence of Usp2 is responsible for the observed phenotype (Fig. 5B). Taken together, these data demonstrate that Usp2 is transcriptionally responsive to growth phase and stringent response inducers and required for growth in the presence of stringent stress.

Usp2 does not contribute to staphylococcal pathogenesis in a systemic animal model of infection

The abundance of Usp2 in the staphylococcal kidney abscess indicates that this protein might play a role in the host-pathogen interaction. To test the contribution of Usp2 to staphylococcal pathogenesis, cohorts of 6–8 week old female C57BL/6 mice were systemically infected with wildtype Newman, Δ*usp2*, or Δ*usp2* containing a full-length copy of *usp2* expressed in trans (Δ*usp2*/p*lgt-usp2-c-myc*). To allow comparisons between these

three strains, Newman and Δ*usp2* were transformed with an empty vector pOS1-plgt [18]. Ninety-six hours post infection, the mice were sacrificed and kidneys were removed, homogenized, and bacteria were enumerated. These experiments demonstrated that there is no significant difference between wildtype and Δ*usp2* at colonizing murine kidneys (Fig. 6A). To determine if the role of Usp2 during pathogenesis is affected by strain background, the Δ*usp2* mutation was transduced into the MRSA strain USA300 and both wildtype and the Δ*usp2* mutant were tested in the systemic model of infection. Again no significant difference was observed between the two groups (Fig. 6B). These results indicate that despite the apparent abundance of Usp2 in the staphylococcal abscess, the Usp2 protein is dispensable for the pathogenesis of *S. aureus* in the model of infection tested in this study. Further analyses of proteins contained within the abscess are necessary to determine which factors are critical to the host-pathogen interaction.

Discussion

S. aureus is a leading cause of global morbidity and mortality and is associated with abscess formation in a variety of vertebrate hosts. Abscesses are inflammatory lesions containing accumulated bacteria surrounded by both necrotic and healthy immune cells comprised primarily of polymorphonuclear leukocytes, or neutrophils [3,19]. Although the contribution of individual staphylococcal proteins to abscess development and maintenance has been evaluated, a comprehensive analysis of the composition of a staphylococcal abscess at the molecular level is still lacking [19,20]. Such an analysis should reveal the factors that contribute to abscess formation and uncover host and bacterial factors that are critical to the outcome of the host-pathogen interaction.

The bacterial factors that are expressed during infection are not well defined; however, recent developments in proteomics combined with the unique anatomical structure of the abscess provide the opportunity to identify proteins expressed specifically at the site of infection [21]. Laser capture microdissection (LCM) allows the precise acquisition of specific cell populations of interest from heterogeneous tissue sections [22,23]. Additionally, the development of liquid chromatography tandem mass spectrometry (LC-MS/MS) permits the analysis of hundreds to thousands of proteins directly from a complex protein mixture with a sensitivity that can reach sub-femtomole levels [24]. Coupling LCM with LC-MS/MS technology enables the proteomic analysis of a single infection site with exceptional sensitivity [25].

The majority of experiments evaluating the staphylococcal proteome have compared wildtype and isogenic mutants of *S. aureus* or have monitored the impact of altered *in vitro* conditions on protein abundance [26,27,28]. Ventura *et al.*, utilized proteomics to study the host-pathogen interface in a murine model of staphylococcal pneumonia [29]. In the current study, proteins were detected directly within kidney abscesses. Despite the fact that the majority of the proteins detected were from the mammalian host, the staphylococcal proteins identified in this analysis represent a number of known virulence factors and resulted in the identification of previously uncharacterized staphylococcal proteins such as Usp2.

The universal stress protein superfamily (Pfam accession number PF00582) encompasses a conserved group of proteins that are present within bacteria, archaea, fungi, insects and plants [14]. There is significant variation in the *usp* copy number across organisms that encode this protein, ranging from one to fourteen copies within an individual genome [14,30]. *S. aureus* strain Newman contains two genes *NWMN_1600* and *NWMN_1604* that encode Usp1 and Usp2, respectively [31]. We have found that Usp2 is abundant in the staphylococcal abscess, yet it is not required for bacterial survival in a systemic model of infection. In *E. coli,* Usp expression is induced by exposure to an array of stresses including nutrient starvation, elevated temperatures, oxidants, electron transport chain uncouplers, and antibiotics [32,33,34]. In the case of *Salmonella typhimurium,* UspA contributes to virulence in mice [15]. Conversely, *M. tuberculosis* strains inactivated for the universal stress protein homolog Rv2623 fail to establish chronic tuberculosis infection in guinea pigs and mice, exhibiting a hypervirulent phenotype associated with increased bacterial burden and mortality [35]. These findings have led to the suggestion that Rv2623 is an ATP-dependent signaling intermediate in a pathway that promotes persistent infection [35]. The *S. aureus usp2* gene increases expression upon exposure to stringent stress [17]. Additionally, it has been reported that a fragment of *S. aureus* Usp2 protein has adhesive properties towards some host molecules such as fibronectin and fibrinogen [36]. It is unclear how to accommodate this finding with the predicted cytoplasmic localization of Usp2, however it only adds to the potential role that this protein might play at the host-pathogen interface. The inability to detect a difference in the colonization capabilities of Δ*usp2* in two strain backgrounds highlights the importance of further characterizing members of the abscess proteome, and suggests redundancy in the staphylococcal mechanisms used for survival within the host.

The host proteins identified in the staphylococcal abscess included a number of known neutrophil proteins. This includes the nuclear protein histone H4 which acts as a scaffold for the formation of NETs to trap and kill pathogens [11,12]. The presumed extracellular localization of H4 in the abscess emphasizes the posthumous killing mechanisms of the neutrophil and caused us to explore the potential antimicrobial role of this basic protein. Purified human histone H4 has been shown to have antimicrobial activity against *S. aureus* [37], however this analysis was performed using a Δ*mprF* mutant that exhibits increased sensitivity to cationic peptides [38]. In the current study, we report antimicrobial activity of H4 against the wildtype *S. aureus* strain Newman, indicating that H4 is included in the antimicrobial arsenal of the neutrophils.

Several components of the clotting cascade were identified in *S. aureus*-infected tissues from neutropenic mice. *S. aureus* is known to bind to and manipulate components of the vertebrate clotting and fibrinolytic cascades, including fibrinogen, prothrombin, and plasminogen. We identified the alpha, beta, and gamma chains of fibrinogen as enriched in infected lesions from neutropenic mice relative to non-neutropenic mice. Of the staphylococcal proteins identified in these lesions, two (Ssp/Emp and MapN/Eap) are known to have fibrinogen-binding properties and contribute to abscess formation and persistence [39,40,41]. Passive immunization with antibodies directed to these two proteins was previously found to decrease staphylococcal burdens in tissues from systemically-infected

mice [41]. Thus, our results provide further evidence that *S. aureus* interacts with clotting and fibrinolytic cascade components at the infectious interface.

There are important limitations to this study. Proteomic analysis of abscessed tissues identified predominantly host proteins, and only a limited number of bacterial proteins. While this may reflect the current technological limits of mass spectrometry-based protein detection in histologic samples, the failure to identify additional bacterial proteins in abscessed tissues might also be a function of the relatively small proportion of bacterial cells relative to host cells within an abscess. A previous ultrastructual characterization of abscess architecture revealed that at days 4–5 post-inoculation, staphylococci coalesce into central, densely packed communities to comprise only a small percentage of abscess volume [41]. A second limitation of this work is the inability to discern whether staphylococcal proteins enriched in neutropenic lesions are more abundantly produced in the absence of neutrophils, or simply reflect higher bacterial burdens in an immunocompromised mouse. However, this approach facilitated the identification of additional staphylococcal proteins not detected in the abscesses of wildtype mice. Whether production of these bacterial proteins represents a specific adaptation to infected tissues in neutropenic hosts remains to be tested. Finally, we were unable to identify a role for Usp2 in staphylococcal survival within infected organs. It is possible that Usp2 has a more prominent role in staphylococcal pathogenesis in neutropenic mice. Alternatively, Usp2 may contribute to staphylococcal pathogenesis specifically within abscesses, an effect potentially masked by enumeration of bacterial burdens from entire organs containing a mixture of abscessed and non-abscessed tissues.

In conclusion, this work identifies the proteins present within staphylococcal kidney abscesses. Expanding this analysis to abscesses caused by other bacteria, or staphylococcal abscesses from additional infection sites will begin to define how abscess composition differs across infections. Moreover, uncovering host and bacterial factors that contribute to the outcome of infection may potentiate the design of new intervention measures to treat this important infectious threat.

Materials and Methods

Ethics Statement

All procedures involving animals were approved by Vanderbilt University's Institutional Animal Care and Use Committee (IACUC).

Bacterial strains and growth conditions

Staphylococcus aureus clinical isolate Newman [31] was used in all experiments (wildtype) and mutants were generated in its background, unless otherwise indicated. *S. aureus* was grown on tryptic soy broth (TSB) solidified with 1.5 % agar at 37°C or in TSB with shaking at 180 rpm. When needed, TSB was supplemented with antibiotics to the following final concentrations: chloramphenicol (10 μg ml-1) and spectinomycin (100 μg ml-1). *Escherichia coli* was grown in Luria broth (LB) and when appropriate, the media were supplemented with antibiotics as follows: ampicillin (100 μg ml-1), kanamycin (40 μg ml-1) and spectinomycin (100 μg ml-1).

Construction of Δ*usp2* isogenic mutants

Primers AA531 (5′-GGGGACAAGTTTGTACAAAAAAGCAGGCTGTCGAAGTACGCGGTACTGCACCTGGC ATAT-3′, attB1 site underlined) and AA529 (5′-GTCCCGGGAGTAAGTGCCTCCTTGTT-3′, XmaI site underlined) were used to amplify the upstream region of the *usp2* ORF (*NWMN_1604*) and primers AA530 (5′-AACCCGGGATATAGATGATCATTAGA-3′, XmaI site underlined) and AA532 (5′-GGGGACCACTTTGTACAAGAAAGCTGGGTCCATAAATTTGTATCACAAAGAGCGGC AGAA-3′, attB2 site underlined) were used to amplify the region downstream of the *usp2* ORF. Both PCR amplicons were ligated into the vector pCR2.1 (Invitrogen). The resulting plasmid was digested with XmaI and ligated to the non-polar spectinomycin cassette from plasmid pSL60-1[42]. The PCR fragment containing the flanking regions and the spectinomycin resistance cassette was then amplified and recombined into pKOR1 [43]. The Δ*usp2::spc* mutant was constructed in strain Newman by allelic replacement as described [43]. The Newman strain mutation was then transduced into the MRSA strain USA300[44] with phage Φ85[45].

Creation of strains for complementation of Δ*usp2*

The *usp2* ORF was PCR-amplified using the primers AA526 (5′-CATATGATTACTTACAAAAATAT-3′, NdeI site underlined) and AA534 (5′-GGATATCAGTTTCTGTTCGCCGCCATTTTGATATTTTTCACGTAATTGAGTTGTT-3′, EcoRV site underlined), digested with NdeI and EcoRV, then ligated into the vector p*hrtB-myc* [46] replacing the *hrtB* ORF with the *usp2* ORF. The resulting plasmid was designated p*lgt-usp2-c-myc*. This plasmid was transformed into the restriction-deficient modification-positive *S. aureus* RN4220 and subsequently transformed into Δ*usp2* for analyzing the infectivity of this mutant in the systemic model of infection (see below). To construct a plasmid expressing the *usp2* gene under the control of its native promoter, a 300 nucleotide region containing the putative *usp2* promoter was PCR-amplified using the primers AA528 (5′-CGAATTCTTTGTAATCTACATCTT-3′, EcoRI site underlined) and AA542 (5′-GTAAGTCATATGAGTAAGTGCCTCCTTGTTCTTT-3′, NdeI site underlined), digested with EcoRI and NdeI, then ligated into p*lgt-usp2-c-myc* that had been digested with the same restriction enzymes. The resulting plasmid was designated p*usp2-c-myc* and was used for complementation of the Δ*usp2* mutant in the stringent stress assay (see below). As a control, both wildtype Newman and Δ*usp2* were transformed with the *E. coli*/*S. aureus* shuttle vector pOS1-p*lgt* [18].

Construction of transcriptional reporters

(A) *xylE* reporter: To construct a *usp2-xylE* transcriptional reporter, a 300 nucleotide region directly upstream of the predicted translational start site of the *usp2* ORF was amplified with primers AA528 and AA541 (5′-TGAATTCAGTAAGTGCCTCCTTGTTCTTT-3′, EcoRI site underlined), then digested with EcoRI and ligated into pOS1-*xylE* [47] that had been digested with EcoRI. (B) *gfp* reporter: To construct a *usp2-gfp* transcriptional reporter, the same region described in (A) was amplified with primers AA538 (5′-GCACTGCAGTTCTTTGTAATCTACATCTT-3′, PstI site underlined), and AA539 (5′-

GTGGTACCAGTAAGTGCCTCCTTGTTCTTT-3′, KpnI site underlined), and digested with PstI and KpnI then ligated upstream of the *gfp* gene in the vector pAH842 [48] that had been digested with the same restriction enzymes.

Transcriptional reporter assays

(A) XylE assay: Bacterial cultures were grown overnight in 15 ml conical tubes then diluted 1:100 into fresh media. Aliquots were removed at time intervals corresponding to the different growth phases (mid-log phase: 3 hrs and OD_{600}~ 0.3, late log phase: 6 hrs and OD_{600}~ 0.6, early stationary phase: 8 hrs and OD_{600}~ 0.7, and late stationary phase; 24 hrs and OD_{600}~ 0.65). Cells in each aliquot were washed and frozen until the time of analysis. The XylE assay was performed as described previously [47]. Briefly, cells were lysed using 100 mM potassium phosphate buffer (pH 8.0), 10% (vol vol-1) acetone, and lysostaphin (25 mg ml-1) for 20 min at 37°C. Cells debris was removed by centrifugation at 20,000 g for 30 min at 4°C. Supernatants were assayed for XylE activity by monitoring the formation of 2-hydroxymuconic semialdehyde from pyrocatechol through measuring the absorbance at 375 nm every minute for 30 min on a Synergy 2 Multi-Mode Microplate Reader (Biotek). Protein concentration in each sample was determined by BCA (Pierce). One unit of specific activity of XylE in a sample is defined as the formation of 1 nmol of 2-hydroxymuconic semialdehyde per minute per milligram of cellular protein [49]. Each experiment was performed in triplicate and repeated three times. (B) GFP assay: Bacterial cultures were grown overnight at 37°C with shaking then diluted 1:100 in 5 ml of fresh medium and allowed to grow for 90 min at 37°C with shaking. Cells were then pelleted by centrifugation and resuspended in 4 ml of TSB ± mupirocin (60 μg ml-1) and allowed to grow for 60 min at 37°C with shaking. Aliquots of 200 μl were removed, placed in clear bottom 96-well plate and fluorescence was measured using a Synergy 2 Multi-Mode Microplate Reader (Biotek). For normalization of the samples, the absorbance of the same wells was measured at 600 nm. Normalized fluorescence was expressed as fold change in fluorescence as compared to the mupirocin untreated sample. Each experiment was performed in triplicate and repeated three independent times.

Stringent stress assay

The ability of *S. aureus* to resist the stringent stress induced by mupirocin was assessed by the use of a liquid-phase assay. Briefly, overnight bacterial cultures were diluted in TSB to a final concentration of approximately 1×10^5 to 2×10^5 CFU/ml. Subsequently, 20 μl aliquots were added to 180 μl of TSB with 120 μg ml-1 mupirocin or TSB with an equivalent volume of absolute ethanol which was used as a vehicle to dissolve the mupirocin. The mixtures were incubated at 37°C for 15 min without shaking, then 20 μl aliquots were removed, diluted 10-fold and plated on TSA plates. After incubation at 37°C overnight, the colonies were enumerated and the percentage of survival was determined by comparing the CFUs from the mupirocin-treated cultures to those treated with vehicle alone. Each experiment was performed in duplicate and repeated three independent times.

Histone (H4) growth inhibition assay

To assess the growth inhibitory activity of histone (H4), overnight cultures of wildtype *S. aureus* were diluted 1:30 in Roswell Park Memorial Institute (RPMI) medium supplemented

with 1% (wt vol-1) Casamino Acids (CAS) to which purified human histone H4 (New England Laboratories) was added in 2-fold increasing concentrations (0.78 to 100 μg ml-1). As a negative control, cells were grown in RPMI/CAS to which equivalent volumes of H4 buffer (20 mM sodium phosphate (pH 7.0), 300 mM NaCl, 1 mM EDTA, and 1 mM DDT) were added. Cell suspensions were incubated in round bottom 96 well plates at 37°C with shaking at 180 rpm. Bacterial growth was monitored by measuring absorbance at 600 nm.

Murine model of infection

Analyzing the infectivity of Δusp2—Six- to eight-week-old female C57BL/6 mice (Jackson Laboratories, Bar Harbor, Maine) were infected retro-orbitally with approximately 1×10^7 CFU of *S. aureus* NW/pOS1-*lgt*, NWΔ*usp2*/pOS1-*lgt*, and NWΔ*usp2*/p*lgt-usp2-c-myc*. Ninety-six hours post-infection, mice were euthanized with CO_2, kidneys were removed, homogenized in sterile PBS, serially diluted and plated on TSA and TSA/10 μg ml-1 chloramphenicol for colony forming unit (CFU) counts. The experiment was also performed using USA300 WT and USA300 *Δusp2*, with plating on TSA.

Infections for shotgun proteomics—These infections were performed essentially as described above however, twenty-four hours prior to the infection, mice were injected intraperitoneally with 250 μg of either anti-Gr1 antibody (RB6) or isotype control (SRF3). On the day of infection, a second dose of the antibodies was administered. Mice treated with RB6 were infected with 1×10^6 CFU as opposed to those treated with SRF3 which were infected with 1×10^7 CFU. The difference in the bacterial inocula between the two groups is due to the expected higher susceptibility of the neutropenic mice (RB6-treated) to *S. aureus.* After euthanization, kidneys were either flash frozen in liquid nitrogen (for laser capture micro dissection) or fixed in formalin (for histology and immunohistochemistry).

Histology and immunohistochemistry

Following overnight fixation in formalin, the kidneys were processed routinely, embedded in paraffin, and sectioned at five microns. Sections were stained with hematoxylin and eosin for microscopic evaluation. Additional unstained tissue sections were deparaffinized and processed for immunohistochemistry with rabbit polyclonal anti-sera against myeloperoxidase (MPO-7, Dako) and histone H4 (ab61255, Abcam). Diaminobenzidine was used as the substrate. Detailed information on immunohistochemistry protocols can be found at the following website, http://www.mc.vanderbilt.edu/root/vumc.php?site#tpsr

Excising abscessed tissue using laser capture microdissection (LCM)

Frozen kidneys were sliced into 5 μm sections and placed on a histology glass slide. Samples were fixed in ethanol and xylene then air-dried for 5 minutes. Tissues in three separate abscessed regions from one representative anti-RB6 treated (neutropenic) mouse, and one representative anti-SRF3 treated (isotype control) mouse were microdissected at 10x and 40x magnification, and with a power range of 70 mW – 100 mW and pulse range 2,500 μs – 11,000 μs using automated LCM (Veritas System). The abscessed tissues were captured on LCM caps and removed from the machine and kept frozen until further analyses. The abscesses were less obvious in the neutropenic mice; however ethanol and xylene treatment of the sections revealed the margins of the deformed tissues allowing the

accurate microdissection of the lesioned tissue. Thirty microliters of 25 μg mL-1 lysostaphin in TBS was placed on the membrane of each LCM cap and incubated at 37°C for 30 min. This lysostaphin treatment was intended to dissolve the bacterial cell wall to increase sensitivity of the detection of bacterial proteins. After digestion, the caps were inverted and placed into 200 μL microcentrifuge tubes and the lysates collected by centrifugation for 1 minute at 16,100 × g. The lysates from lysostaphin-treated caps were then combined and solubilized in SDS sample buffer and equally distributed into 3 lanes and the proteins were resolved by electrophoresis on a 10–20% Tricine gel. The gels were stained with Colloidal Blue with destaining with water and each lane was cut into 5 gel regions. The proteins were then subjected to in-gel trypsin digestion and peptide extraction digestion using a standard protocol [50]. Briefly, the gel regions were washed with 100 mM NH_4HCO_3 for 15 minutes. The liquid was discarded and replaced with fresh 100 mM NH_4HCO_3 and the proteins reduced with 5 mM DTT for 20 minutes at 55°C. After cooling to room temperature, iodoacetamide was added to 10 mM final concentration and placed in the dark for 20 minutes at room temperature. The solution was discarded and the gel pieces washed with 50% acetonitrile/50 mM NH_4HCO_3 for 20 minutes, followed by dehydration with 100% acetonitrile. The liquid was removed and the gel pieces were completely dried, re-swelled with 0.5 μg of modified trypsin (Promega) in 100 mM NH_4HCO_3, and digested overnight at 37°C. Peptides were extracted by three changes of 60% acetonitrile/0.1% TFA, and all extracts were combined and dried *in vacuo*. Samples were reconstituted in 30 μL 0.1 % formic acid for LC-MS/MS analysis.

The membranes containing the LCM material were removed, placed directly into a 1.5 mL Eppendorf tube and suspended in 25 μL of SDS sample buffer, reduced with DTT and heated at 70–80°C in a water bath for 10 min. The supernatants from the caps treated with SDS were combined, equally distributed into 9 wells and electrophoresed approximately 2 cm into a 10–20% Tricine gel. All gels were stained with Colloidal Blue with destaining with water and each region was digested as described above. The peptide digests from 3 abscessed or lesioned regions were combined resulting in 3 technical replicates.

Liquid chromatography tandem mass spectrometry (LC-MS/MS) analysis of abscessed tissues

Peptides were analyzed using a Thermo Finnigan LTQ ion trap instrument and separated as previously described [51]. Tandem spectra were acquired using a data dependent scanning mode with a one full MS scan (*m/z* 400–2000) followed by 9 MS-MS scans. The SEQUEST algorithm was then used to search the tandem spectra against the C57BL/6 mouse and *S. aureus* Newman genomes. The database was concatenated with the reverse sequences of all proteins in the database to allow for the determination of false positive rates. The SEQUEST outputs were filtered through the IDPicker suite with a false positive ID threshold of 5% and proteins were required to be identified by 2 or more unique peptides. Protein reassembly from identified peptide sequences was done as previously described [52]. The number of spectra identified for each protein under a given condition was normalized to the number of total spectra detected in the same injection. The spectral counts for each protein were derived from three technical replicates, representing laser-captured tissue from three separate abscessed or lesioned regions.

Statistical Analysis

Student's *t* test was used to calculate *p* values, and *p* values less than 0.05 were considered significant.

Acknowledgments

We thank members of the Skaar lab for critical reading of the manuscript. This work was supported by NIH grant U54 AI057157 from the Southeastern Regional Center of Excellence for Emerging Infections and Biodefense and grants AI073843 and AI069233 from NIAID. EPS is a Burroughs Wellcome Fund Investigator in the Pathogenesis of Infectious Disease.

References

1. Lowy FD. *Staphylococcus aureus* infections. N Engl J Med. 1998; 339:520–532. [PubMed: 9709046]
2. Klevens RM, Morrison MA, Nadle J, Petit S, Gershman K, et al. Invasive methicillin-resistant *Staphylococcus aureus* infections in the United States. JAMA. 2007; 298:1763–1771. [PubMed: 17940231]
3. Cheng AG, DeDent AC, Schneewind O, Missiakas D. A play in four acts: *Staphylococcus aureus* abscess formation. Trends Microbiol. 2011; 19:225–232. [PubMed: 21353779]
4. Czuprynski CJ, Brown JF, Maroushek N, Wagner RD, Steinberg H. Administration of anti-granulocyte mAb RB6-8C5 impairs the resistance of mice to *Listeria monocytogenes* infection. Journal of immunology. 1994; 152:1836–1846.
5. Hestdal K, Ruscetti FW, Ihle JN, Jacobsen SE, Dubois CM, et al. Characterization and regulation of RB6-8C5 antigen expression on murine bone marrow cells. Journal of immunology. 1991; 147:22–28.
6. Corbin BD, Seeley EH, Raab A, Feldmann J, Miller MR, et al. Metal chelation and inhibition of bacterial growth in tissue abscesses. Science. 2008; 319:962–965. [PubMed: 18276893]
7. Wolffe AP, Guschin D. Review: chromatin structural features and targets that regulate transcription. J Struct Biol. 2000; 129:102–122. [PubMed: 10806063]
8. Parseghian MH, Luhrs KA. Beyond the walls of the nucleus: the role of histones in cellular signaling and innate immunity. Biochem Cell Biol. 2006; 84:589–604. [PubMed: 16936831]
9. Jacobsen F, Baraniskin A, Mertens J, Mittler D, Mohammadi-Tabrisi A, et al. Activity of histone H1.2 in infected burn wounds. J Antimicrob Chemother. 2005; 55:735–741. [PubMed: 15772144]
10. Howell SJ, Wilk D, Yadav SP, Bevins CL. Antimicrobial polypeptides of the human colonic epithelium. Peptides. 2003; 24:1763–1770. [PubMed: 15019208]
11. Ermert D, Urban CF, Laube B, Goosmann C, Zychlinsky A, et al. Mouse neutrophil extracellular traps in microbial infections. J Innate Immun. 2009; 1:181–193. [PubMed: 20375576]
12. Brinkmann V, Reichard U, Goosmann C, Fauler B, Uhlemann Y, et al. Neutrophil extracellular traps kill bacteria. Science. 2004; 303:1532–1535. [PubMed: 15001782]
13. Marchler-Bauer A, Lu S, Anderson JB, Chitsaz F, Derbyshire MK, et al. CDD: a Conserved Domain Database for the functional annotation of proteins. Nucleic acids research. 2011; 39:D225–229. [PubMed: 21109532]
14. Kvint K, Nachin L, Diez A, Nystrom T. The bacterial universal stress protein: function and regulation. Curr Opin Microbiol. 2003; 6:140–145. [PubMed: 12732303]
15. Liu WT, Karavolos MH, Bulmer DM, Allaoui A, Hormaeche RD, et al. Role of the universal stress protein UspA of *Salmonella* in growth arrest, stress and virulence. Microb Pathog. 2007; 42:2–10. [PubMed: 17081727]
16. Crosse AM, Greenway DL, England RR. Accumulation of ppGpp and ppGp in *Staphylococcus aureus* 8325–4 following nutrient starvation. Lett Appl Microbiol. 2000; 31:332–337. [PubMed: 11068918]

17. Anderson KL, Roberts C, Disz T, Vonstein V, Hwang K, et al. Characterization of the *Staphylococcus aureus* heat shock, cold shock, stringent, and SOS responses and their effects on log-phase mRNA turnover. J Bacteriol. 2006; 188:6739–6756. [PubMed: 16980476]
18. Bubeck Wardenburg J, Williams WA, Missiakas D. Host defenses against *Staphylococcus aureus* infection require recognition of bacterial lipoproteins. Proc Natl Acad Sci U S A. 2006; 103:13831–13836. [PubMed: 16954184]
19. Cheng AG, Kim HK, Burts ML, Krausz T, Schneewind O, et al. Genetic requirements for *Staphylococcus aureus* abscess formation and persistence in host tissues. FASEB J. 2009; 23:3393–3404. [PubMed: 19525403]
20. Tzianabos AO, Wang JY, Lee JC. Structural rationale for the modulation of abscess formation by *Staphylococcus aureus* capsular polysaccharides. Proc Natl Acad Sci U S A. 2001; 98:9365–9370. [PubMed: 11470905]
21. Francois P, Scherl A, Hochstrasser D, Schrenzel J. Proteomic approaches to study *Staphylococcus aureus* pathogenesis. J Proteomics. 2010; 73:701–708. [PubMed: 19879388]
22. Bonner RF, Emmert-Buck M, Cole K, Pohida T, Chuaqui R, et al. Laser capture microdissection: molecular analysis of tissue. Science. 1997; 278:1481–1483. [PubMed: 9411767]
23. Rekhter MD, Chen J. Molecular analysis of complex tissues is facilitated by laser capture microdissection: critical role of upstream tissue processing. Cell Biochem Biophys. 2001; 35:103–113. [PubMed: 11898852]
24. Washburn MP, Wolters D, Yates JR 3rd . Large-scale analysis of the yeast proteome by multidimensional protein identification technology. Nat Biotechnol. 2001; 19:242–247. [PubMed: 11231557]
25. Liao L, Cheng D, Wang J, Duong DM, Losik TG, et al. Proteomic characterization of postmortem amyloid plaques isolated by laser capture microdissection. J Biol Chem. 2004; 279:37061–37068. [PubMed: 15220353]
26. Singh VK, Jayaswal RK, Wilkinson BJ. Cell wall-active antibiotic induced proteins of *Staphylococcus aureus* identified using a proteomic approach. FEMS Microbiol Lett. 2001; 199:79–84. [PubMed: 11356571]
27. Wolf C, Hochgrafe F, Kusch H, Albrecht D, Hecker M, et al. Proteomic analysis of antioxidant strategies of *Staphylococcus aureus*: diverse responses to different oxidants. Proteomics. 2008; 8:3139–3153. [PubMed: 18604844]
28. Resch A, Leicht S, Saric M, Pasztor L, Jakob A, et al. Comparative proteome analysis of *Staphylococcus aureus* biofilm and planktonic cells and correlation with transcriptome profiling. Proteomics. 2006; 6:1867–1877. [PubMed: 16470655]
29. Ventura CL, Higdon R, Hohmann L, Martin D, Kolker E, et al. *Staphylococcus aureus* elicits marked alterations in the airway proteome during early pneumonia. Infect Immun. 2008; 76:5862–5872. [PubMed: 18852243]
30. O'Toole R, Williams HD. Universal stress proteins and *Mycobacterium tuberculosis*. Res Microbiol. 2003; 154:387–392. [PubMed: 12892844]
31. Duthie ES, Lorenz LL. Staphylococcal coagulase; mode of action and antigenicity. J Gen Microbiol. 1952; 6:95–107. [PubMed: 14927856]
32. Nachin L, Nannmark U, Nystrom T. Differential roles of the universal stress proteins of *Escherichia coli* in oxidative stress resistance, adhesion, and motility. J Bacteriol. 2005; 187:6265–6272. [PubMed: 16159758]
33. Gustavsson N, Diez A, Nystrom T. The universal stress protein paralogues of *Escherichia coli* are co-ordinately regulated and co-operate in the defence against DNA damage. Mol Microbiol. 2002; 43:107–117. [PubMed: 11849540]
34. Nystrom T, Neidhardt FC. Expression and role of the universal stress protein, UspA, of *Escherichia coli* during growth arrest. Mol Microbiol. 1994; 11:537–544. [PubMed: 8152377]
35. Drumm JE, Mi K, Bilder P, Sun M, Lim J, et al. *Mycobacterium tuberculosis* universal stress protein Rv2623 regulates bacillary growth by ATP-Binding: requirement for establishing chronic persistent infection. PLoS Pathog. 2009; 5:e1000460. [PubMed: 19478878]

36. Kylvaja R, Kankainen M, Holm L, Westerlund-Wikstrom B. Adhesive polypeptides of *Staphylococcus aureus* identified using a novel secretion library technique in *Escherichia coli*. BMC Microbiol. 2011; 11:117. [PubMed: 21615970]
37. Lee DY, Huang CM, Nakatsuji T, Thiboutot D, Kang SA, et al. Histone H4 is a major component of the antimicrobial action of human sebocytes. J Invest Dermatol. 2009; 129:2489–2496. [PubMed: 19536143]
38. Kristian SA, Durr M, Van Strijp JA, Neumeister B, Peschel A. MprF-mediated lysinylation of phospholipids in *Staphylococcus aureus* leads to protection against oxygen-independent neutrophil killing. Infect Immun. 2003; 71:546–549. [PubMed: 12496209]
39. Hussain M, Becker K, von Eiff C, Schrenzel J, Peters G, et al. Identification and characterization of a novel 38.5-kilodalton cell surface protein of *Staphylococcus aureus* with extended-spectrum binding activity for extracellular matrix and plasma proteins. Journal of bacteriology. 2001; 183:6778–6786. [PubMed: 11698365]
40. Lee LY, Miyamoto YJ, McIntyre BW, Hook M, McCrea KW, et al. The *Staphylococcus aureus* Map protein is an immunomodulator that interferes with T cell-mediated responses. The Journal of clinical investigation. 2002; 110:1461–1471. [PubMed: 12438444]
41. Cheng AG, Kim HK, Burts ML, Krausz T, Schneewind O, et al. Genetic requirements for *Staphylococcus aureus* abscess formation and persistence in host tissues. The FASEB journal: official publication of the Federation of American Societies for Experimental Biology. 2009; 23:3393–3404. [PubMed: 19525403]
42. Lukomski S, Hoe NP, Abdi I, Rurangirwa J, Kordari P, et al. Nonpolar inactivation of the hypervariable streptococcal inhibitor of complement gene (sic) in serotype M1 *Streptococcus pyogenes* significantly decreases mouse mucosal colonization. Infect Immun. 2000; 68:535–542. [PubMed: 10639414]
43. Bae T, Schneewind O. Allelic replacement in *Staphylococcus aureus* with inducible counter-selection. Plasmid. 2006; 55:58–63. [PubMed: 16051359]
44. Tenover FC, Goering RV. Methicillin-resistant *Staphylococcus aureus* strain USA300: origin and epidemiology. The Journal of antimicrobial chemotherapy. 2009; 64:441–446. [PubMed: 19608582]
45. Mazmanian SK, Skaar EP, Gaspar AH, Humayun M, Gornicki P, et al. Passage of heme-iron across the envelope of *Staphylococcus aureus*. Science. 2003; 299:906–909. [PubMed: 12574635]
46. Attia AS, Benson MA, Stauff DL, Torres VJ, Skaar EP. Membrane damage elicits an immunomodulatory program in *Staphylococcus aureus*. PLoS Pathog. 2010; 6:e1000802. [PubMed: 20300601]
47. Torres VJ, Stauff DL, Pishchany G, Bezbradica JS, Gordy LE, et al. A *Staphylococcus aureus* regulatory system that responds to host heme and modulates virulence. Cell Host Microbe. 2007; 1:109–119. [PubMed: 18005689]
48. Malone CL, Boles BR, Lauderdale KJ, Thoendel M, Kavanaugh JS, et al. Fluorescent reporters for *Staphylococcus aureus*. J Microbiol Methods. 2009; 77:251–260. [PubMed: 19264102]
49. Chien Y, Manna AC, Projan SJ, Cheung AL. SarA, a global regulator of virulence determinants in *Staphylococcus aureus*, binds to a conserved motif essential for sar-dependent gene regulation. J Biol Chem. 1999; 274:37169–37176. [PubMed: 10601279]
50. Ham AJ, Caprioli RM, Gross ML. Proteolytic Digestion Protocols. In The Encyclopedia of Mass Spectrometry Volume. 2005; 2:10–17.
51. Tabb DL, Fernando CG, Chambers MC. MyriMatch: highly accurate tandem mass spectral peptide identification by multivariate hypergeometric analysis. J Proteome Res. 2007; 6:654–661. [PubMed: 17269722]
52. Zhang B, Chambers MC, Tabb DL. Proteomic parsimony through bipartite graph analysis improves accuracy and transparency. J Proteome Res. 2007; 6:3549–3557. [PubMed: 17676885]

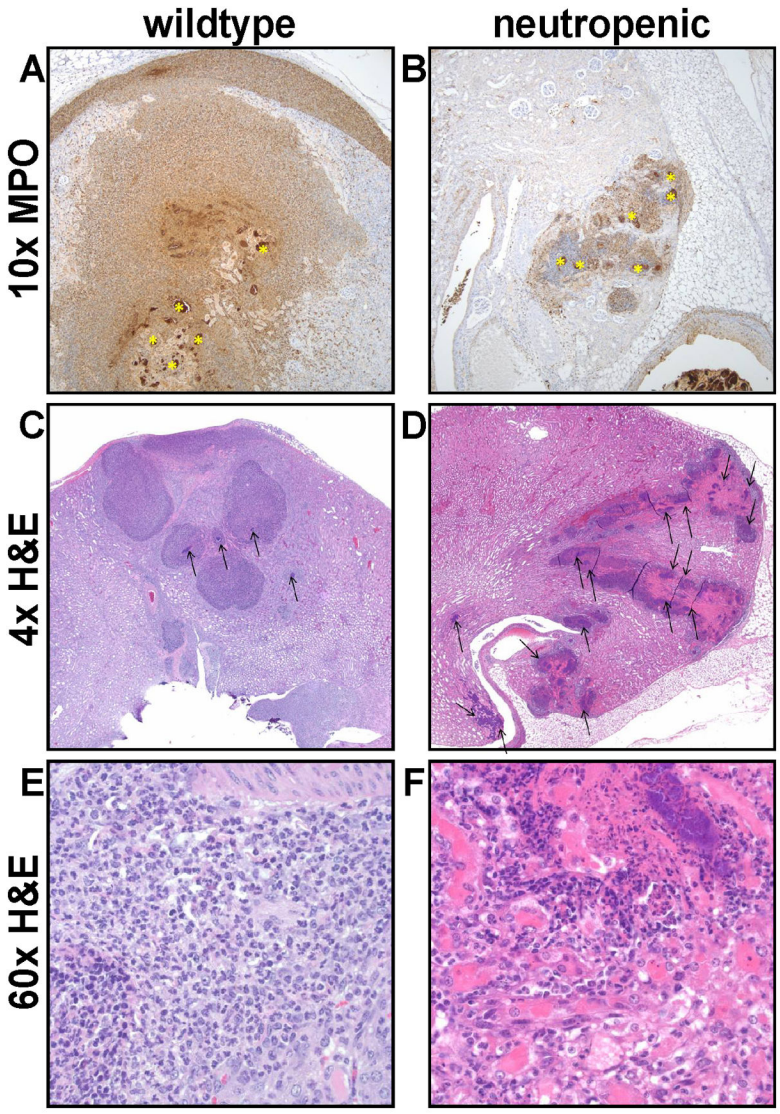

Figure 1. Neutrophil depletion results in large, disorganized renal lesions

(A and B) 10x magnification of immunohistochemistry for myeloperoxidase from a mouse treated with (A) the control antibody (SRF-3) or (B) the anti-Gr1 RB6 antibody. A substantial decrease in the number of neutrophils infiltrating and surrounding the bacteria in the neutropenic mice is observed and marked (*). (C) 4x magnification of H & E stained sections of the wildtype mouse where the inflammatory infiltrate consists of both neutrophils and macrophages forming densely packed sheets that encircle small bacterial aggregates (arrows) while the neutropenic mouse (D) has large, disorganized lesions and the inflammatory infiltrate consists predominantly of macrophages and abundant bacterial growth is visible (arrows). (E and F) 60x magnification of the sections described in (C) and (D), respectively.

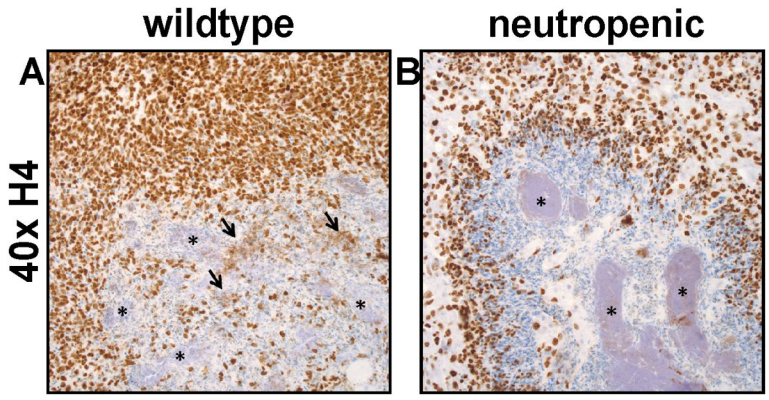

Figure 2. Histone H4 is decreased upon neutrophil depletion

(A and B) Immunohistochemistry for histone H4. (A) In the SRF3-treated mouse (wildtype), there is increased extracellular immunoreactivity for histones (arrows) in proximity to the bacterial cells (*). (B) Anti-Gr1(RB6)-treated mice (neutropenic) have fewer infiltrating cells, very little extracellular histone H4, and large bacterial aggregates (*).

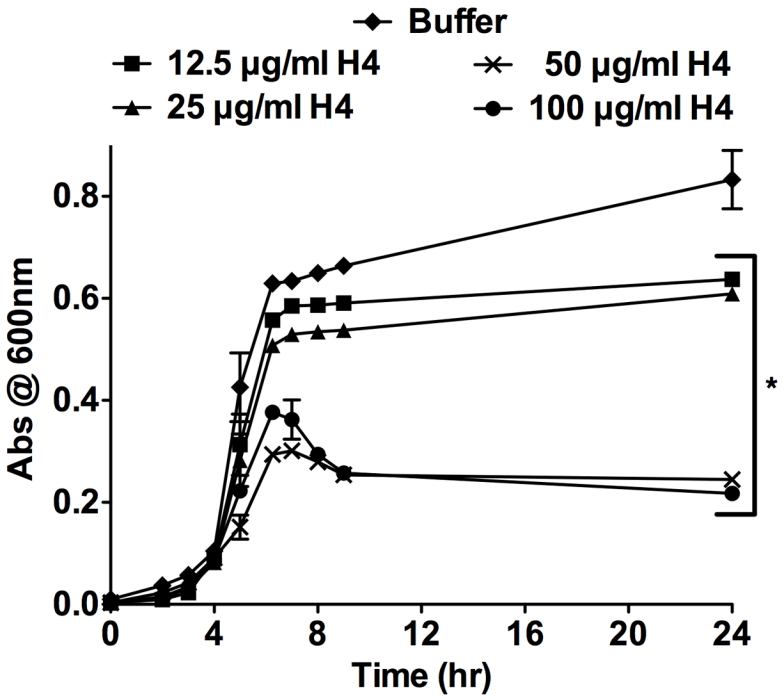

Figure 3. Histone H4 inhibits *S. aureus* growth *in vitro*

S. aureus was cultured in the presence of increasing concentrations of purified histone H4. The growth of the bacterial cells was monitored by measuring the optical density of the cultures at 600 nm. The data presented are the average of two independent experiments, each performed in triplicate. Error bars represent the standard error. * Denotes $p < 0.01$ versus buffer control as calculated by Student's *t* test.

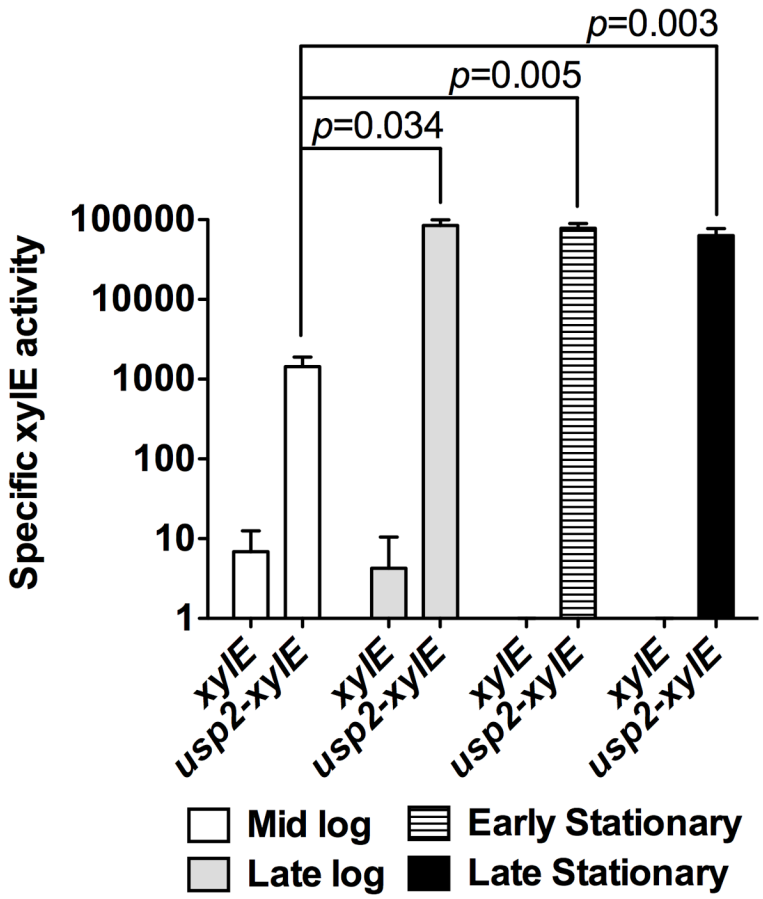

Figure 4. Expression of *usp2* is growth phase-dependent

XylE assay for *usp2* promoter activity. *S. aureus* containing a promoterless *xylE* construct (*xylE*) or *xylE* downstream of the *usp2* promoter (*usp2-xylE*) were grown to the indicated growth phases and specific XylE activity was determined. The data presented are the average of three independent experiments, each one performed in triplicate, and the error bars represent the standard error. Student's *t* test was used to calculate *p* values.

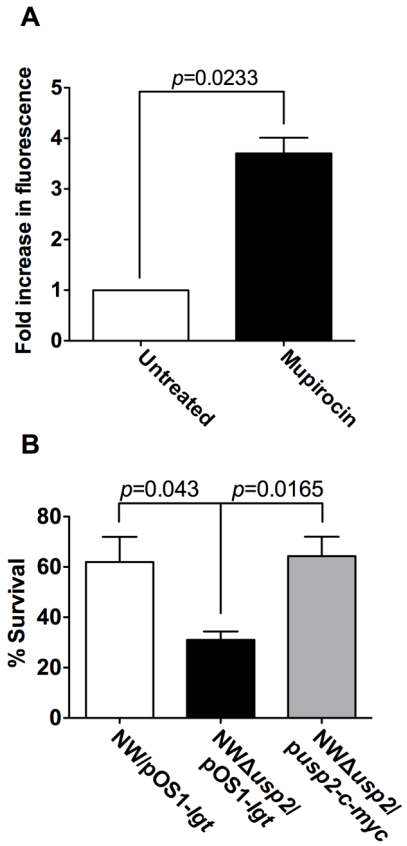

Figure 5. Expression of *usp2* is induced during the stringent response

(A) The *usp2* promoter was fused to GFP and fluorescence was used as a measurement of *usp2* expression when exposed to mupirocin at a final concentration of 60 μg ml-1. The data are presented as fold increase in fluorescence as compared to the reporter exposed to the vehicle control. The data presented are the average of three independent experiments each performed in triplicate, and the error bars represent the standard error. B) Bacterial survival assay: wildtype NW/pOS1-*lgt*, NWΔ*usp2*/pOS1-*lgt* and NWΔ*usp2*/p*usp2-c-myc* were incubated with or without 120 μg ml-1 mupirocin and the percent survival was calculated by considering the number of bacteria present in the absence of mupirocin as 100%. The data presented are the average of three independent experiments each performed in triplicate, and the error bars represent the standard error. Student's *t* test was used to calculate *p* values.

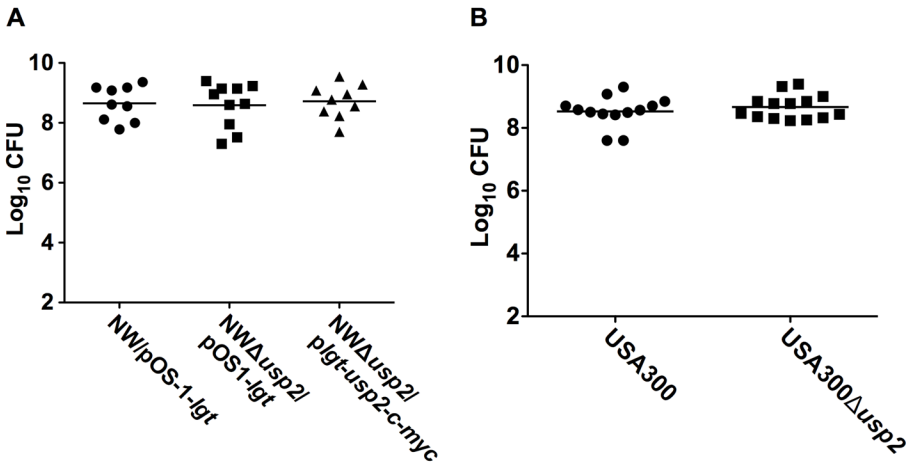

Figure 6. Usp2 does not contribute to *S. aureus* pathogenesis in the systemic model of infection

Bacterial colony forming units (CFU) measured in kidneys from mice intravenously infected with (A) wildtype NW/pOS1-*lgt* (circles), NWΔ*usp2*/pOS1-*lgt* (squares), and NWΔ*usp2*/p*lgt-usp2-c-myc* (triangles). (B) wildtype USA300 (circles) or Δ*usp2* (squares). Each mouse is represented by a data point in the figure and the horizontal bar represents the mean of the $\log_{10}$CFU.

Table 1

Summary of the number of proteins detected in the abscesses of *S. aureus* infected mice.

	Neu > WT	**Neu < WT**	**Neu ≈ WT**	**Total**
S. aureus	13	0	9	22
Mouse	38	40	237	315
Totals	51	40	246	337

“Neu” indicates RB6-treated mice.

“WT” indicates SRF-3 treated mice.

>Indicates that the numbers of peptides detected were significantly higher.

<Indicates that the numbers of peptides detected were significantly lower.

≈Indicates that the numbers of peptides detected were not significantly different.

Table 2

Mouse proteins less abundant in *S. aureus*-infected mouse abscesses from neutropenic mice as compared to wildtype mice.

Protein[a]	Neu[b]		WT[c]		Neu/WT[f]	*p* value[g]
	Mean[d]	SD[e]	Mean[d]	SD[e]		
Innate Immunity						
Myeloid bactenecin (Neutrophilic granule protein)	24	12.75	295	33.99	0.08	0.0034
Lactotransferrin precursor	67	45.00	278	47.77	0.24	0.0044
Annexin A1	53	13.40	218	23.58	0.24	0.0162
Lysozyme C type M precursor	41	10.59	186	23.43	0.22	0.0033
Myeloperoxidase	67	15.48	135	24.28	0.49	0.0121
Neutrophil gelatinase-associated lipocalin precursor	17	10.71	120	32.24	0.14	0.0303
Lymphocyte cytosolic protein 1	12	2.86	62	0.00	0.20	0.0366
CD177 antigen	9	3.32	52	5.17	0.17	0.0258
Leukocyte elastase precursor	5	5.14	38	0.00	0.14	0.0020
Cathelin-related antimicrobial peptide precursor	0	0.00	35	6.37	0.00	0.0116
S100-A11	2	3.01	30	5.52	0.06	0.0359
Antioxidants						
Peroxiredoxin-5	45	8.94	149	17.30	0.30	0.0001
Cytoskeleton and ECM						
Myosin heavy chain IX	145	14.56	334	8.63	0.43	0.0002
Filamin, alpha	18	8.35	107	9.01	0.16	0.0009
Integrin alpha M	2	3.25	59	0.00	0.03	0.0098
Integrin beta-2 precursor	5	5.21	51	0.00	0.10	0.0018
Lamin-B receptor	5	0.27	27	0.00	0.19	0.0083
Talin-1	5	5.64	25	0.00	0.22	0.0141
Actin related protein 2/3 complex	0	0.00	6	0.00	0.00	0.0002
Histones						
Histone 4	**349**	**35.50**	**722**	**141.44**	**0.48**	**0.0262**
Hist1h2bj protein	135	29.69	365	44.21	0.37	0.0149

Protein[a]	Neu[b]		WT[c]		Neu/WT[f]	*p* value[g]
	Mean[d]	SD[e]	Mean[d]	SD[e]		
Histone cluster 1, H3g	31	14.60	67	15.63	0.46	0.0457
Heterogeneous nuclear ribonucleoprotein C	0	0.00	21	5.98	0.00	0.0268
General Cell Processes						
Alpha-enolase	81	21.19	171	43.41	0.48	0.0404
Aldo-keto reductase family 1, member A4	57	7.28	149	11.70	0.39	0.0009
Nucleoside diphosphate kinase A	15	5.09	55	3.19	0.28	0.0258
Phosphoglycerate mutase 1	14	5.36	39	7.03	0.35	0.0167
Phosphogluconate dehydrogenase	13	3.78	36	0.00	0.35	0.0242
NADH dehydrogenase (ubiquinone) Fe-S protein 1	5	5.14	19	0.00	0.27	0.0415
Miscellaneous						
Chitinase 3-like protein 3 precursor	195	17.21	388	28.58	0.50	0.0005
Kidney-specific protein homolog	102	10.18	224	46.92	0.45	0.0291
Peptidyl-prolyl cis-trans isomerase A	53	8.03	148	29.75	0.36	0.0456
Rho GDP-dissociation inhibitor 2	23	12.10	99	21.34	0.23	0.0030
Selenium binding protein 1	21	12.02	69	10.72	0.30	0.0113
14–3–3 protein zeta/delta	19	7.48	53	3.35	0.36	0.0061
Guanine nucleotide binding protein, alpha inhibiting 2	12	2.67	32	0.00	0.39	0.0182
Myeloblastin precursor	3	5.67	16	5.17	0.21	0.0488
Rpl30 protein	3	2.99	13	3.18	0.26	0.0144
RAN, member RAS oncogene family	2	3.01	11	0.00	0.16	0.0370
Guanine nucleotide binding protein, alpha inhibiting 3	0	0.00	11	0.00	0.00	0.0342

[a] Protein identification based on UniRef and NCBI database searches.

[b] Neutropenic mouse.

[c] Wildtype mouse.

[d] Mean of the number of spectra detected in the three technical replicate samples analyzed for this condition.

[e] Standard deviation among the number of the spectra detected in the three technical replicate samples analyzed for this condition.

[f] Ratio of the mean of the number of spectra detected in the neutropenic mouse to that in the wildtype mouse.

[g] *p*-value as obtained by applying Student's *t*-test.

Table 3

Mouse proteins more abundant in *S. aureus*-infected mouse abscesses from neutropenic mice as compared to wildtype mice.

Protein[a]	Neu[b]		WT[c]		Neu/WT[f]	*p* value[g]
	Mean[d]	SD[e]	Mean[d, h]	SD[e]		
Clotting Cascade						
Serum amyloid A-1 protein precursor	29	6.32	1	0.00	28.87	0.0156
Serum amyloid A 2	18	5.79	1	0.00	17.70	0.0338
Inter alpha-trypsin inhibitor, heavy chain 4	98	6.27	5	4.63	19.03	0.0001
Plasminogen	96	21.03	6	0.16	15.08	0.0180
Beta-2-glycoprotein 1	24	4.82	3	5.17	7.94	0.0072
Fibrinogen, alpha polypeptide	316	25.33	79	13.71	3.98	0.0007
Alpha-1-antitrypsin 1–5 precursor	23	2.14	8	3.61	2.70	0.0076
Fibrinogen beta chain precursor	574	31.05	257	20.71	2.23	0.0003
Fibrinogen, gamma polypeptide	427	41.61	202	23.58	2.11	0.0032
Kininogen 1	46	12.51	12	10.51	3.88	0.0239
CoA synthesis						
2,4-dienoyl-CoA reductase	9	3.32	1	0.00	8.94	0.0430
Acyl-Coenzyme A oxidase 1	44	9.86	13	6.68	3.41	0.0146
Medium-chain specific acyl-CoA dehydrogenase	32	3.93	13	6.04	2.53	0.0141
Enoyl-Coenzyme A, hydratase	108	10.34	44	6.71	2.44	0.0017
Long-chain specific acyl-CoA dehydrogenase	35	7.25	15	4.08	2.37	0.0217
Cytoskeleton and ECM						
Collagen alpha-1(I) chain precursor	5	0.27	1	0.00	5.33	0.0008
Keratin, type I cytoskeletal	116	23.99	26	2.03	4.52	0.0221
Arpc4 protein	19	2.34	6	0.16	2.99	0.0110
Heat shock						
Heat shock protein 1 (chaperonin)	69	7.37	17	16.36	4.05	0.0182
Heat shock protein, A	40	1.91	16	9.05	2.43	0.0406
Innate Immunity						

Protein[a]	Neu[b]		WT[c]		Neu/WT[f]	*p* value[g]
	Mean[d]	SD[e]	Mean[d, h]	SD[e]		
Complement C3 precursor	161	39.03	73	20.44	2.21	0.0401
Miscellaneous						
Solute carrier family 4 (anion exchanger), member 1	5	0.27	1	0.00	5.33	0.0008
ATP synthase subunit g, mitochondrial	5	0.27	1	0.00	5.33	0.0008
Cytochrome c oxidase subunit VIb isoform 1	20	1.72	1	0.00	20.49	0.0023
3′ (2′), 5′-bisphosphate nucleotidase 1	10	0.86	1	0.00	10.25	0.0023
Kynurenine aminotransferase II	25	9.09	1	0.00	25.04	0.0412
Proteasome	7	2.81	1	0.00	7.04	0.0492
3-hydroxybutyrate dehydrogenase	7	2.81	1	0.00	7.04	0.0492
Prohibitin 2	21	4.41	4	7.29	5.03	0.0356
Ceruloplasmin	133	37.31	32	24.42	4.18	0.0228
Solute carrier family 27 (Fatty acid transporter)	52	10.42	13	0.33	4.08	0.0228
Protein disulfide isomerase associated 3	68	17.55	19	14.46	3.64	0.0212
Prohibitin	14	3.51	4	3.61	3.42	0.0256
Aldehyde dehydrogenase 4 family	29	4.57	8	3.46	3.39	0.0046
UDP-glucuronosyltransferase 1–7 precursor	14	2.47	4	3.61	3.38	0.0216
Ubiquinol-cytochrome c reductase core protein 1	43	7.82	16	3.61	2.71	0.0146
Serine (or cysteine) peptidase inhibitor, clade A	148	26.27	57	33.11	2.57	0.0228
ATP synthase D chain	18	2.55	8	3.46	2.10	0.0234

[a] Protein identification based on UniRef and NCBI database searches.

[b] Neutropenic mouse.

[c] Wildtype mouse.

[d] Mean of the number of spectra detected in the three technical replicate samples analyzed for this condition.

[e] Standard deviation among the number of the spectra detected in the three technical replicate samples analyzed for this condition.

[f] Ratio of the mean of the number of spectra detected in the neutropenic mouse to that in the wildtype mouse.

[g] *p*-value as obtained by applying Student's *t*-test.

[h] In cases where proteins were not detected, a value of 1 was assigned to enable ratio calculation.

Table 4

Staphylococcal proteins enriched in neutrophil-depleted abscesses

Protein[a]	Short name	Newman gene number	WT[b]		Neu[c]		Neu/WT[f]	*p* value[g]
			Mean[d, h]	SD[e]	Mean[d]	SD[e]		
Glycolysis/gluconeogenesis								
Alcohol dehydrogenase	Adh1	NWMN_0577	9	5.14	124	23.41	13.28	0.0012
L-lactate dehydrogenase 2	Ldh	NWMN_2499	8	3.61	25	9.09	2.96	0.0425
Enolase	Eno	NWMN_0745	1	0.00	24	5.18	23.77	0.0014
Glyceraldehyde 3-phosphate dehydrogenase 1	GapA	NWMN_0741	2	3.58	10	0.86	4.96	0.0184
Secreted virulence proteins								
Leukocidin LukE precursor	LukE	NWMN_1719	1	0.00	78	5.01	77.93	0.0000
Leukocidin/hemolysin toxin	LukS	NWMN_1928	6	6.31	62	10.89	9.84	0.0016
Gamma-hemolysin	HlgC	NWMN_2319	2	3.64	45	9.55	21.50	0.0019
MapN protein	MapN (Eap)	NWMN_1872	17	7.84	39	2.33	2.29	0.0097
Leukocidin LukD precursor	LukD	NWMN_1718	1	0.00	35	15.40	34.87	0.0172
Gamma hemolysin,	HlgB	NWMN_2320	1	0.00	31	7.05	31.08	0.0016
Extracellular matrix and plasma binding protein	Ssp (Emp)	NWMN_0758	1	0.00	5	0.27	5.33	0.0000
Stress								
Universal stress protein	Usp2	NWMN_1604	1	0.00	24	4.55	23.79	0.0008
Iron acquisition								
Iron-binding protein IsdA	IsdA	NWMN_1041	3	5.17	24	5.18	7.96	0.0079

[a] Protein identification based on UniRef and NCBI databases searches.

[b] Wildtype mouse.

[c] Neutropenic mouse.[4]

[d] Mean of the number of spectra detected in the three technical replicate samples analyzed for this condition.

[e] Standard deviation among the number of the spectra detected in the three technical replicate samples analyzed for this condition.

[f] Ratio of the mean of the number of spectra detected in the neutropenic mouse to that in the wildtype mouse.

[g] *p*-value as obtained by applying Student's *t*-test.

[h] In cases where proteins were not detected, a value of 1 was assigned to enable ratio calculation.